Since January 2020 Elsevier has created a COVID-19 resource centre with free information in English and Mandarin on the novel coronavirus COVID-19. The COVID-19 resource centre is hosted on Elsevier Connect, the company's public news and information website.

Biosensors and Bioelectronics 202 (2022) 113978

Contents lists available at ScienceDirect

Biosensors and Bioelectronics

journal homepage: www.elsevier.com/locate/bios

SARS-CoV-2 detection using quantum dot fluorescence immunochromatography combined with isothermal amplification and CRISPR/Cas13a

Qin Zhang [a,1], Jiahao Li [b,1], Yue Li [b], Guolei Tan [a], Mei Sun [a], Yanke Shan [b], Yue Zhang [b], Xin Wang [b], Keyu Song [a], Rui Shi [a], Ling Huang [a], Fei Liu [b,**], Yongxiang Yi [a,***], Xuping Wu [a,*]

[a] The Second Hospital of Nanjing, Nanjing University of Chinese Medicine, Nanjing, Jiangsu, 210003, China
[b] Joint International Research Laboratory of Animal Health and Food Safety of Ministry of Education & Single Molecule Nanometry Laboratory (Sinmolab), Nanjing Agricultural University, Nanjing, Jiangsu, 210095, China

ARTICLE INFO

Keywords:
SARS-CoV-2
CRISPR/Cas13a
Quantum dot fluorescence immune-chromatography
Isothermal amplification

ABSTRACT

The development of reliable, sensitive, and fast devices for the diagnosis of COVID-19 is of great importance in the pandemic of the new coronavirus. Here, we proposed a new principle of analysis based on a combination of reverse transcription and isothermal amplification of a fragment of the gene encoding the S protein of the SARS-CoV-2 and the CRISPR/Cas13a reaction for cleavage of the specific probe. As a result, the destroyed probe cannot be detected on an immunochromatographic strip using quantum fluorescent dots. Besides, the results can be obtained by an available and inexpensive portable device. By detecting SARS-CoV-2 negative (n = 25) and positive (n = 62) clinical samples including throat swabs, sputum and anal swabs, the assay showed good sensitivity and specificity of the method and could be completed within 1 h without complicated operation and expensive equipment. These superiorities showed its potential for fast point-of-care screening of SARS-CoV-2 during the outbreak, especially in remote and underdeveloped areas with limited equipment and resources.

1. Introduction

Coronavirus disease 2019 (COVID-19), the disease associated with severe acute respiratory syndrome coronavirus 2 (SARS-CoV-2), first reported in December 2019, in Wuhan, China, has caused a severe pandemic worldwide in the past two years (Wang et al., 2020b; Zhu et al., 2020). To this day, the pandemic has not been effectively contained and continues to place a huge burden on global public health and social welfare (Laborde et al., 2020; Nicola et al., 2020; WHO, 2021). SARS-CoV-2 is a cunning virus that infects the body with the common symptoms of upper respiratory tract infection, including fever, cough and fatigue, making it difficult to distinguish it from other seasonal respiratory diseases (Huang et al., 2020; Nicholson, 1992; Wang et al., 2020d). In some cases, there were even no clinical signs and symptoms after infection, such individuals were called asymptomatic carriers (Bai et al., 2020; Meyerowitz et al., 2021; Rothe et al., 2020). However, particles shed from them can hang around in the air and inadvertently spread to people with underlying diseases or the elderly (Kevadiya et al., 2021; Wang et al., 2020a; Williamson et al., 2020). Therefore, early detection of infectors helps CDC to carry out epidemiological investigations, track the source of transmission and take effective measures.

The widespread development and promotion of multiple tests for effective and rapid testing in the event of an outbreak remain a key point in the fight against the COVID-19 pandemic (Pinheiro et al., 2021). Antibodies and antigen tests based on lateral flow type assays are commonly used (Hou et al., 2020a; Mak et al., 2020; Yuce et al., 2021). However, antibodies are the result of the body's response to the virus and cannot be used as a direct indicator of infection diagnosis. Moreover, the body needs enough time to produce antibodies at detectable levels and this pervasive delayed response leads to false negatives (Yuce et al., 2021). Antigen tests lack specificity due to antigens

* Corresponding author.
** Corresponding author.
*** Corresponding author.
E-mail addresses: feiliu24@njau.edu.cn (F. Liu), yongxiangyi@njucm.edu.cn (Y. Yi), xuping.wu@njucm.edu.cn (X. Wu).
[1] The two authors contribute equally.

https://doi.org/10.1016/j.bios.2022.113978
Received 15 November 2021; Received in revised form 5 January 2022; Accepted 6 January 2022
Available online 10 January 2022

well-conserved among different coronavirus species (Kevadiya et al., 2021). The rapid spread of viruses in human populations poses a challenge to rapidly developing molecular diagnostic methods in clinical diagnostic laboratories. Real-time reverse transcription-polymerase chain reaction (RT-PCR), droplet digital polymerase chain reaction (ddPCR), next-generation sequencing (NGS), reverse transcription loop-mediated isothermal amplification (RT-LAMP), clustered regularly interspaced short palindromic repeats (CRISPR)/Cas-based point-of-care testing techniques and other detection methods have been successively developed and applied to SARS-CoV-2 detection to facilitate the early identification of infected persons (Broughton et al., 2020; CDC, 2020; Chaibun et al., 2021; Chiara et al., 2021; Corman et al., 2020; Deiana et al., 2020; Fozouni et al., 2021; Kevadiya et al., 2021; Thi et al., 2020). RT-PCR, based on viral gene fragments and recommended by the World Health Organization (WHO) and the American CDC, is currently the most widespread method for COVID-19 detection (CDC, 2020; WHO, 2020). However, the special need for sophisticated instruments and professionals, as well as the high cost, make it difficult to popularize RT-PCR in remote and underdeveloped areas like Africa (Kevadiya et al., 2021). Similar limitations exist for ddPCR and NGS applied and popularized in remote regions (Chiara et al., 2021; Deiana et al., 2020). In response to the limitations posed by the abovementioned methods and the shortage of RT-PCR reagents, new platforms and diagnosis methods are actively being pursued. Biosensor-based detection methods are also being developed, in which the electronic signals generated by the combination of biological receptors and analytes are used to identify viruses and other analytes (Karkan et al., 2022; Pinheiro et al., 2021). However, these biosensor methods still suffer from low sensitivity (Karkan et al., 2022).

Here, we report a CRISPR/Cas13a-based fluorescent nanoparticle SARS-CoV-2 (CFNS) assay and perform a coincidence rate experiment with a commercial RT-PCR kit. To our knowledge, this is the first study combining a Cas13a-based nucleic acid test strip with quantum dot microspheres (QDM_S) for assaying SARS-CoV-2, as shown in Fig. 1A and B. During the whole experiment, in Fig. 1A and B, the extracted nucleic acids were firstly amplified by reverse-transcription recombinase-aided amplification (RT-RAA) at 39 °C for 25min. By RT-RAA reaction, RNA was reversely transcribed into cDNA and then amplified to obtain sufficient target nucleic acid. Then, the amplified products were specifically recognized and cleaved through the CRISPR/Cas13 reaction. Moreover, the cleavage products and sheep anti-FITC IgG antibody-labeled QDM (QDM-anti-FITC antibody) were mixed and added to the test strip for 15 min. Finally, the fluorescence intensity values of the T-line and the C-line could be obtained to calculate the fluorescence ratio by using the miniature intelligent fluorescence detector (Fig. 1C). It is worth noting that all clinical samples used in this study were treated in strict accordance with the standard operation for SARS-CoV-2 by the standard diagnostic pipeline of the hospital laboratory in Fig. 1D. In summary, our proposed detection method has good specificity, sensitivity, and repeatability, and can be used for epidemiologic surveys.

2. Materials and methods

2.1. DNA/RNA in the assay preparation

The nucleic acid sequence for the RT-RAA and Cas13a cleavage reaction was designed by Zhang et al. against the S genes. We chose the conserved area of S genes, and the selected sequence was not in the range of S protein key mutation sites D614G, T478K, P681R, and L452R. RT-RAA primers (F and R), positive standard DNA template, sgRNA and reporter probe were obtained from Sangon Biotech (Shanghai, China). Standard positive synthetic RNA was transcribed with positive standard

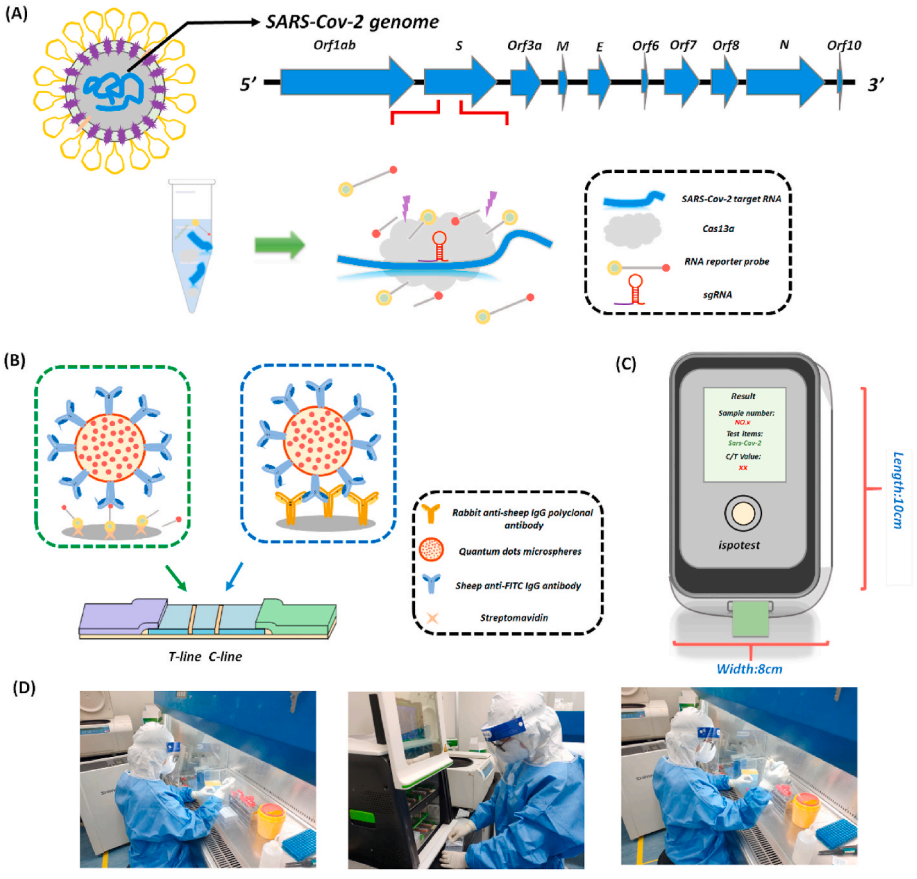

Fig. 1. Schematic and characterization of CFNS sensor. (A) Amplification and cleavage reaction target of the CFNS detection method. (B) Ultrasensitive Immunochromatographic assay of SARS-CoV-2 with QDMs. (C) Miniaturized intelligent fluorescence reader. (D) CFNS assay in a front-line hospital in Nanjing.

DNA as a template using an In Vitro Transcription T7 Kit (Takara Bio Inc., China) and purified and recovered with a Spin Column RNA Cleanup & Concentration Kit (Sangon Biotech, Shanghai, China) according to the manufacturer's instructions. All the obtained RNA fragments were aliquoted and stored at −80 °C until use. All DNA/RNA sequences used in this assay are listed in Table S1. RT-RAA kit was obtained from Qitian Biotech (Jiangsu, China). Streptavidin was obtained from Sigma-Aldrich (USA), and anti-FITC antibody was obtained from Abcam (UK). QDMs were obtained from Kundao Biotech (Shanghai, China).

2.2. Collection of clinical samples

This study was approved by the medical ethics committee of the Second Hospital of Nanjing (2020-LS-ky014). Clinical positive samples (throat swabs, n = 37; sputum, n = 20; anal swabs, n = 5) were from patients with SARS-CoV-2-positive infection based on clinical symptoms and signs, chest imaging, serological tests and epidemiological evidence. In addition, clinical negative (throat swabs, n = 25) and interfering samples (n = 85), viruses including those with *adenovirus (ADV), rhinovirus (HRV), respiratory syncytial virus (RSV), Epstein-Barr virus (EB), cytomegalovirus (CMV), varicella-zoster virus (VZV), influenza A (H7N9) virus (AIV-H7N9), hepatitis B virus (HBV), hepatitis C virus (HCV), human immunodeficiency virus (HIV), New Bunia virus (SFTSV)*, and bacteria including *Mycobacterium tuberculosis (MTB)* and *nontuberculous mycobacteria (NTM), Klebsiella pneumoniae (KP), Acinetobacter baumannii (ABA), Mycoplasma pneumoniae (MP),* and *Pseudomonas aeruginosa (PA)* were collected by the Second Hospital of Nanjing (Detailed information were provided as shown in Tables S2 and S3).

2.3. Validation of the collected clinical samples

Clinical positive samples (throat swabs, sputum and anal swabs) were first inactivated in a water bath at 56 °C for 30 min for biosecurity reasons, and then nucleic acid extraction was performed on a fully automatic nucleic acid extractor (Jiangsu perBiotechnology Co., Ltd.). For sputum samples, equal volume of sputum digestive juice (0.78 g NaCl and 0.1 g DTT in100 mL PBS) was added, working for 10–20 min to liquefy sputum. For thick sputum, more DTT could be added as appropriate to make the sputum fully liquefied. Finally, RT-PCR assays for SARS-CoV-2 were performed using a clinically validated kit approved by the Chinese National Medical Products Administration, Food and Drug Administration (FDA) and Conformite European certification (Sansure Biotech, Changsha, China and BGI.Dx, Shenzhen, China) on an ABI-7500 Real-Time PCR System (Thermo Fisher Scientific, Carlsbad, CA) according to the instructions, with Ct values below 40 considered positive. Other interfering samples (*ADV, HRV, RSV, EB, CMV, VZV, AIV-H7N9, HBV, HCV, HIV, SFTSV, MTB, NTM, KP, ABA, MP* and *PA*) were determined through laboratory standard testing and analysis methods.

2.4. Preparation of QDM-anti-FITC antibody conjugates

A QDM-anti-FITC antibody was fabricated based on procedures described in previous literature, with slight modification. In brief, QDM_S (50 μL) were activated first in 1-(3-Dimethylaminopropyl)-3-ethylcarbodiimide hydrochloride (10 mg/mL) and N-Hydroxysuccinimide (10 mg/mL) in 2-morpholinoethanethanesulfonic acid (MES) (100 μL, 0.01 M, pH = 6.0) at 37 °C with continuous shaking for 30 min. Then, QDM_S were separated by centrifugation, and the supernatant was discarded. Afterward, they were dispersed in MES (100 μL, 0.02 M, pH = 7.2) to react with anti-FITC antibody (10 μg) for approximately 4 h at room temperature. After that, the QDM-anti-FITC antibody conjugates were blocked with 10% BSA PBS buffer solution (2 μL, 0.01 M, pH = 7.0) at room temperature with gentle agitation for 20 min. After the end of the blocking, the mixture was centrifuged at 10,000 rpm for 15 min, and the precipitate was resuspended in phosphate buffer (100 μL, 10 mM PB, pH = 7.0) at 4 °C until use.

2.5. Fabrication of fluorescence immunochromatographic strips

Lateral flow biosensors were assembled using our group's previous work, with some modifications, as shown in Fig. 1B, C and S4. A streptavidin (2.5 mg/mL) solution and rabbit anti-sheep IgG polyclonal antibody (0.8 mg/mL) solution were sprayed on a nitrocellulose membrane as the T-line and C-line, respectively. Each immunochromatographic strip was cut into 5 mm wide sections using a cutting machine (JinBio, Shanghai, China), followed by drying in a vacuum drying oven at room temperature overnight.

2.6. RT-RAA and Cas13a cleavage reaction

CFNS assays were achieved using RT-RAA for preamplification of viral RNA targets and Cas13a for the trans-cleavage assay. Additionally, the detection results were obtained on a test strip and miniaturized intelligent instrument. RT-RAA reactions were performed according to the instructions of the RT-RAA nucleic acid amplification kit, with slight modification. Firstly, each reaction containing RT-RAA buffer (6 μL), reverse transcriptase (0.2 μL, 100,000 U/mL), forward and reverse primers (0.5 μL), target RNA (1 μL) and magnesium acetate (2.5 μL) was incubated in a conventional water bath at 39 °C for 25 min. Then, each CRISPR/Cas13a cleavage assay consisting of RT-RAA product (1 μL), 10 × detection buffer (2 μL), sgRNA (1 μL, 10 ng/μL), Cas13a (2 μL), each NTP (0.2 μL), ddH2O (4.6 μL), T7 RNA polymerase (New England Biolabs) (0.6 μL), RNase inhibitor (1 μL), magnesium chloride (6 μL, 20 mM) and reporter probe (1 μL, 20 μM) was also incubated in a conventional water bath at 37 °C for 30 min. After that, PBS (72 μL, 0.01 M, pH = 8.2) and QDM-anti-FITC antibody conjugates (8 μL) were added to the abovementioned cleavage reaction tube and mixed. Finally, the mixture was dropped on the assembled nucleic acid test strip, and the T/C fluorescence ratio was read after 15 min using a miniaturized intelligent fluorescence reader (Fig. S4).

2.7. Evaluation of diagnostic performance and clinical validation

First, the concentration of S gene RNA fragments transcribed in vitro was determined by an ultramicro spectrophotometer (NanoDrop One, Thermo Fisher, USA), and the copy number concentration was then calculated based on the weight and length of the fragment. Serial dilutions with DEPC-treated water were used as templates. Note that to test the accuracy and selectivity of our proposed detection strategy, SARS-CoV-2 clinical samples and interference samples were also tested. In addition, the Ct values of all clinical samples used in this study were determined using real-time fluorescence quantitative PCR.

3. Results

3.1. Characterization of the QDMs and QDM-anti-FITC antibody conjugates

First, high-resolution transmission electron microscopy (TEM, JEOL, Japan) (Fig. 2A and B) images showed that multiple QDMs were successfully encapsulated in the polymer shells and that the QDMs had a relatively uniform size distribution with an average diameter of 100 nm. Then, to characterize the coupling efficiency between QDMs and anti-FITC antibodies, a laser particle size analyzer (Malvern, UK) and TEM were utilized, as shown in Fig. 2C and D. The differences between the edges of the QDMs before and after conjugation were observed by TEM (Fig. 2C and D). As shown in Figs. S1A and S1B, changes in the average hydrodynamic diameter and zeta potential between the QDMs and the conjugated QDMs were observed. The hydrated particle size of antibody coupled QDMs increased, and the zeta potential on the surface of QDMs decreased. The above results proved that the monoclonal antibody was

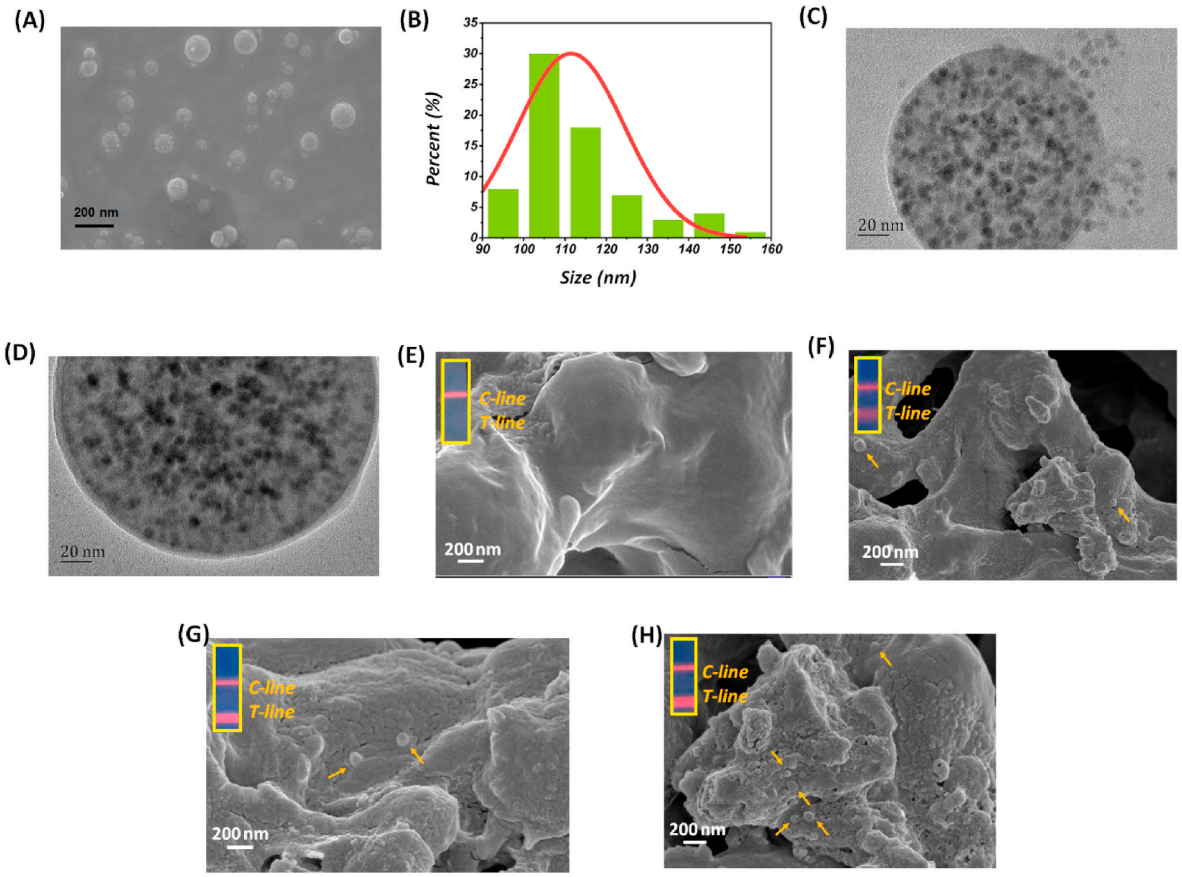

Fig. 2. Verification of CFNS sensor detection performance. (A) SEM images of QDMs. (B) Size distribution histogram of the QDMs. (C) TEM image of the QDMs. (D) TEM image of the QDMs conjugation with anti-FITC antibody. (E) SEM image of the nitrocellulose membrane surface after the modification of streptavidin as well as the addition of 10^{15} Copies per ml SARS-CoV-2 RNA. (F) SEM image of the nitrocellulose membrane surface after the modification of streptavidin as well as the addition of SARS-CoV-2 RNA (Ct = 26). (G) SEM image of the nitrocellulose membrane surface after the modification of streptavidin as well as the addition of SARS-CoV-2 RNA (Ct = 34). (H) SEM image of the nitrocellulose membrane surface after the modification of streptavidin as well as the addition of SARS-CoV-2 negative sample. Arrows indicate QDM-anti-FITC complexes.

successfully assembled on the surface of the QDMs. Additionally, the emission fluorescence spectra of QDMs before and after coupling were measured by a multilabel counter (Tecan, Switzerland), as shown in Fig. S1C. Although the emission intensity of QDM-anti-FITC antibody conjugates was slightly decreased compared with that of QDMs, it is still believed that monoclonal antibody modification did not significantly affect the fluorescence emission performance.

3.2. Development and verification of CFNS sensor

Under optimal experimental conditions, the RT-RAA products were analyzed by 1.5% agarose gel and 2000bp DNA lane was used as marker. The size of the specific band was 121 bp in Fig. S2A, which was consistent with the expected target band size. This indicated that the target RNA was successfully amplified by RT-RAA technology. In addition, after the amplified target RNA was cleaved by the Cas13a enzyme, the cleavage products were analyzed by non-denaturing polyacrylamide gel electrophoresis. Compared with those of the negative control group, the RNA probes of the positive experimental group were cleaved, as shown in Fig. S2B. This result further suggested that sgRNA could specifically recognize the target, thereby activating the "collateral cleavage" function of Cas13a.

According to the principle of the CFNS assays shown in Fig. 1A and B, when the sample under detection contains SARS-CoV-2 nucleic acid, Cas13a binds to the target nucleic acid in the presence of sgRNA and activates the lateral cleavage activity to cleave RNA probes and separates the biotin from FITC. As a result, biotin could not bind to FITC-labeled microspheres after addition. In the capillary migration process, the streptavidin on the T-line could not capture the anti-FITC QDM_S, while the rabbit anti-sheep IgG polyclonal antibody (secondary antibody) on the C-line would combine with the anti-FITC QDM_S to form complexes. On the contrary, when the sample does not contain the target nucleic acid, the RNA probes would not be cleaved, the anti-FITC QDM_S are first bound to the T-line and connected by the RNA probes. Then, the remaining anti-FITC QDM_S are combined with the C-line. Since the content of anti-FITC QDM_S is certain, there is competition between them.

To directly observe the interaction between biotin after sgRNA and Cas13a cleavage, anti-FITC QDM_S and streptavidin on the T-line, the reacted test strips were dried and imaged by scanning electron microscopy (SEM, Hitachi, Japan). According to the previous literature, the surface of the nitrocellulose membrane had a three-dimensional porous network structure, which was convenient for more fully binding with the reporter probe and QDM-anti-FITC complexes. Moreover, as shown in Fig. 2E, F, 2G and 2H, as the number of target nucleic acid copies decreased, more and more reporter probes and QDM-anti-FITC complexes remained on the T-line, resulting in an enhancement of the fluorescence intensity of the T-line and the increase of the T/C fluorescence ratio. The yellow arrow indicated QDM-anti-FITC complexes (similar to spherical shape) in Fig. 2F, G, 2H. The direct observation using SEM showed that the designed test strip has the potential for quantitative SARS-CoV-2 detection.

In this study, we determined the analytical sensitivity of the CRISPR-COVID detection method by performing serial dilutions at various

concentrations. Fig. 3A listed the T/C ratios of standard positive RNA at different concentrations from 10^{15} copies/mL to 1 copy/mL, repeated 5 times for each concentration. The results showed that the CFNS sensor could reach the detection limit of 1 copy/mL according to the cut-off value (0.91) of the proposed detection method. The determination of the cut-off value was the mean and 3SD obtained by measuring 25 clinical negative samples. Additionally, the detection limit was also proven by *t*-test: the p value between the T/C fluorescence ratio with the standard positive RNA concentration of 1 copy/mL and those without standard positive RNA was lower than 0.05. In addition, the standard positive RNA of the same copy number was amplified by the RT-RAA reaction and cut by Cas13a, and the color reaction was performed by a commercial colloidal gold test strip. When the standard positive RNA copy number was 10^4 copies per ml, compared with the negative control, no difference could be observed with the naked eye in Fig. S3. Therefore, we proposed the fluorescence nucleic acid test strips based-QDMs had better stronger signal-to-noise ratio, which could further amplify the detection signal.

3.3. Evaluation of the specificity of CFNS sensors

To confirm the specificity of CFNS sensors in clinical samples, a large number of human pathogens were tested, including (1) common viruses of respiratory infections: *ADV, HRV, RSV, EB, CMV, VZV,* and *AIV-H7N9*; (2) common bacteria of respiratory infections: *MTB* and *NTM, KP, ABA, MP,* and *PA;* and (3) other viruses*: HBV, HCV, HIV,* and *SFTSV*. Based on the detection of 85 interference samples during the experiment, a color map was made by comparing the results obtained with those of positive samples. The histogram on the right showed the change of color as the T/C fluorescence ratio increased. As shown in Fig. 3B, except for the SARS-CoV-2-positive clinical samples, all other pathogen samples were above the detection threshold line, indicating that none of the above-mentioned interfering samples triggered a false positive reaction. In brief, the above experiments suggested that the CFNS sensor we proposed has high specificity and anti-interference ability and could distinguish SARS-CoV-2 from other pathogens of respiratory infections.

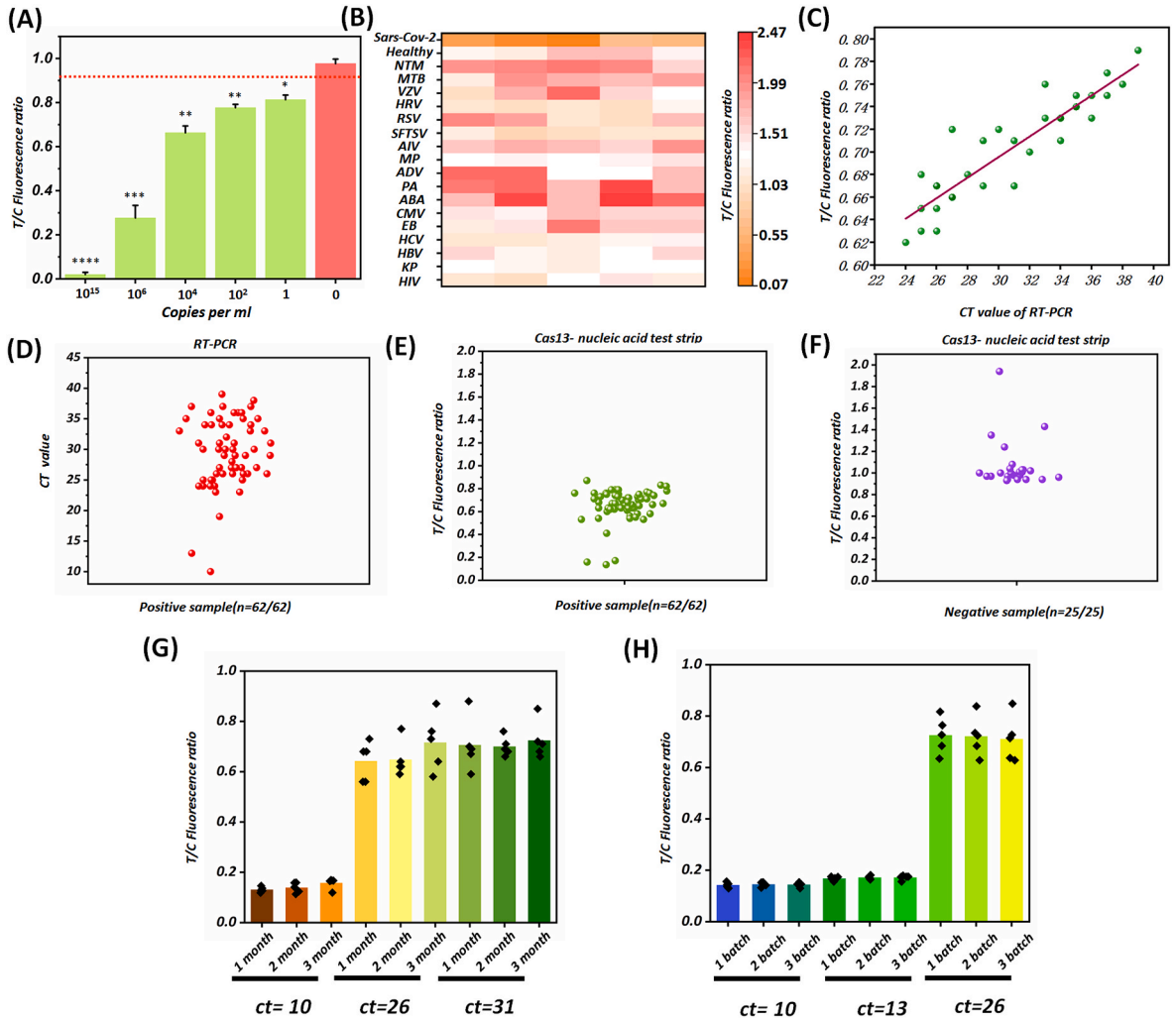

Fig. 3. Evaluation of CFNS sensor detection of clinical samples. (A) Sensitivity analysis of the novel CFNS assay. (B) Specificity evaluation of the proposed CFNS assay method. SARS-CoV-2; Healthy; NTM; MTB; VZV; HRV; RSV; SFTSV; AIV; MP; ADV; PA; ABA; CMV; EB; HCV; HBV; KP; HIV. (C) The correlation analysis of SARS-CoV-2 detection results generated with CFNS assay method and commercial RT-PCR kit. The same sample detection Ct value of commercial RT-PCR kit and the fluorescence ratio of the lateral flow strip were co-analyzed. (D) SARS-CoV-2 positive samples (n = 62) were confirmed through the commercial RT-PCR kit. (E) SARS-CoV-2 positive samples (n = 62) were tested through our proposed CFNS assay method. (F) SARS-CoV-2 negative samples (n = 25) were detected through our proposed CFNS assay method; SARS-COV-2 negative samples were previously determined through commercial RT-PCR kit. (G) Stability test of the CFNS assay in SARS-CoV-2 positive samples at different storage times (1month, 2month, 3month). (H) Verify the stability of the proposed CFNS assay differences between batches (1 batch, 2batch, 3batch) in SARS-CoV-2 positive samples.

3.4. Diagnostic performance of CFNS sensor

After evaluating the analytical performance of the CFNS sensor, the accuracy of the proposed SARS-CoV-2 testing technique in clinical applications was further evaluated. 62 clinically positive samples were tested using the gold standard RT-PCR, and then these samples were also tested using a CFNS sensor. Fig. 3C compared the detection results of clinical positive samples measured by both RT-PCR and the CFNS sensor: all the detection results were located around the line with $r = 0.89$ ($p < 0.05$), indicating the quantified signals at the T/C fluorescence ratio of fluorescence test strips were well correlated with the Ct values from the RT-PCR results.

Moreover, 87 clinical samples including 62 positive samples and 25 negative samples were tested by RT-PCR, and then these samples were also tested by our proposed SARS-CoV-2 testing technique. As the gold standard detection method for the detection of SARS-CoV-2, the RNA extracted from clinical samples was tested in parallel using RT-PCR. A blind taste tests our CFNS sensor could also correctly identify and distinguish 62 positive samples and 25 negative samples in Fig. 3D, E, 3F. Compared with the RT-PCR results shown in Table 1, our proposed CFNS sensor has 100% specificity and 100% sensitivity, and its kappa value is 1.

Next, we performed stability test of the CFNS assay in SARS-CoV-2 positive samples at different storage times (1month, 2month, 3month). As shown in Fig. 3G, these T/C fluorescence ratios were quite close under the same SARS-CoV-2 concentration conditions. This result indicated that the CFNS sensor we proposed could be maintained for 3 months at room temperature and proved that the CFNS assay method had stable detection performance. Finally, to verify the stability of the proposed CFNS test in different batches of strips, these calibrated clinical positive samples were measured by 45 fluorescent test strips from three batches. According to Fig. 3H, the T/C fluorescence ratios corresponding to positive samples with different Ct values 10, 13, and 26, proved its good stability and reproducibility.

4. Discussion

SARS-CoV-2 has ravaged the world for two years and shows no signs of stopping, continuing to place a burden on human lives and the social economy. A variety of laboratory tests based on virus characteristics have been developed and applied in the hospitals, the CDC and the third-party detection institutions. Currently, tests for COVID-19 divide into two main categories: serological and molecular. The former is mainly detected by immunological method of antigen and antibody, while the latter is mainly detected by RT-PCR method of viral nucleic acid (Behera et al., 2021). These methods play an important role in large-scale population screening, differential diagnosis of suspected cases, and evaluation of the treatment effect of patients. Due to the sensitivity and cross-reaction problems, serological tests can only be used as an auxiliary diagnostic means rather than directly for the diagnosis of virus infection. Therefore, nucleic acid detection is still a preferred tactic for SARS-CoV-2 testing, and many nucleic acid-based detection methods have been developed. The American CDC and the European Union recommended the use of real-time quantitative PCR for nucleic acid detection, because of its sensitivity and accuracy, it has become the current mainstream nucleic acid detection method. However, considering the complexity of operation and the shortage of reagents, new rapid and sensitive molecular diagnostic methods are still needed.

Table 1
Concordance between RT–PCR and our proposed CFNS assay method of SARS-CoV-2 RNA among real clinical samples.

Methods		RT-PCR		Total	Kappa
		Positive	Negative		
CFNS sensor	*Positive*	*62*	*0*	*62*	
	Negative	*0*	*25*	*25*	*1*
	Total	*62*	*25*	*87*	

To achieve sensitive and simple molecular detection in any laboratory using ready-made chemical reagents and common equipment, the introduction and availability of CRISPR-based detection technology would accelerate the development of next-generation viral nucleic acid detection technology (Wang et al., 2020f). Broughton et al. developed a CRISPR/Cas12-based lateral flow assay combined with RT-LAMP for detection of SARS-CoV-2 from respiratory swab RNA extracts (Broughton et al., 2020). Fozouni et al. reported the development of an amplification-free CRISPR/Cas13a assay for detecting SARS-CoV-2 directly from nasal swab RNA that can be read with a mobile phone microscope (Fozouni et al., 2021). Zhang et al. combined the Specific High-sensitivity Enzymatic Reporter unlocking (SHERLOCK) system based on CRISPR/Cas13 with colloidal gold test strips recognized by the naked eye for the first time to detect SARS-CoV-2 (Zhang et al., 2020). Next, on the basis of the original detection technology, they further increased the amount of initial RNA in the sample by adding magnetic beads during nucleic acid extraction, thereby improving the detection sensitivity. At the same time, the FDA urgently granted approval to the Sherlock CRISPR SARS-CoV-2 kit, which is the first CRISPR technology-based COVID-19 test approved by the FDA. Since then, an increasing number of research groups have focused on the detection of SARS-CoV-2 based on Cas12a/Cas13a detection technology, as shown in Table 2. Ding et al. developed the All-In-One-Dual CRISPR/Cas12a method to visually detect SARS-CoV-2 and verified its accuracy by testing 28 clinical samples (Ding et al., 2020). Hou et al. established a CRISPR/Cas13a-based isothermal diagnosis method for COVID-19 (Hou et al., 2020b). Most of these methods use colloidal gold test strips for naked-eye color reaction or fluorescence signal reading instruments to collect and analyze fluorescent dyes on RNA/DNA probes.

The application potential of rapid diagnostic technology based on CRISPR/Cas12a/13a is tremendous. With the emergence of quantum dot nanomaterials and miniaturized intelligent sensors, their application potential has increased. Nanomaterial contributes to developing sensitive, rapid and effective diagnostics, providing a viable alternative to RT-PCR for virus detection, which could play a role in a pandemic (Kevadiya et al., 2021). QDMs have the advantages of narrow fluorescence emission spectrum, wide UV excitation, large molar extinction coefficient, high quantum yield and photochemical stability as well as they can be easily functionalized with a series of biological molecules, which make them one of the ideal fluorescent markers (Bruchez et al., 1998; Michalet et al., 2005; Resch-Genger et al., 2008). The combination of QDMs and immunochromatographic test strip can amplify the detectable signal increasing the sensitivity of immunochromatography. In this article, we first extracted viral RNA with a magnetic bead extraction kit in an automatic nucleic acid extraction instrument; then, viral nucleic acids were amplified through RT-RAA and CRISPR/Cas13a cleavage reactions. Second, QDM-anti-FITC antibody conjugates were employed as fluorescent nanoprobes. Compared with ordinary colloidal gold and the fluorescent dye FITC, our fluorescent probe has a higher signal-to-noise ratio, which further amplifies the detection signal. Finally, with a miniaturized intelligent fluorescence analyzer to collect and analyze the amplified fluorescent signal, the detection of a single copy of the SARS-CoV-2 nucleic acid could be achieved within 1 h. Importantly, QDMs combined with RT-RAA and CRISPR/Cas13a amplify the detection signal and improve analytical sensitivity with the help of precise recognition of sgRNA and lateral cleavage activity of Cas13a. We explored the analytical sensitivity by continuous dilution, which could reach 1 copy per ml, and demonstrated that this method could specifically distinguish SARS-CoV-2 from other pathogens. In the whole experiment, apart from the extraction process, devices such as an intelligent miniature testing instrument (~3000 RMB, <500 USD) and a heater (~300 RMB, <50 USD) are still required. Compared to the sophisticated instruments required for RT-PCR and sequencing, the devices we used were simple, inexpensive and easily available.

Table 2
Comparison of the Proposed Sensor with the Reported Methods for SARS-CoV-2 RNA detection.

Sensing principle	*Detection device*	*Amplification*	*LOD*	*Time*	*Reference*
Amplification-free CRISPR/Cas13a	*Mobile phone microscope*	*NO*	*100 copies/mL*	30 min	(Fozouni et al., 2021)
CRISPR/Cas13a test combines RT-RPA	*ABI-7500 Real-Time PCR System*	*RT-RPA*	*7.5 copies/reaction*	40 min	Hou et al. (2020b)
Amplification-free nucleic acid immunoassay	*The supporting fluorescence analysis device*	*NO*	*1000 TU/ml*	*less than 1 h*	(Wang et al., 2020c)
All-In-One Dual CRISPR/Cas12a	*Naked eye under LED light*	*RT-RPA*	*5 copies*	20 min	(Ding et al., 2020)
SHERLOCK assay using Cas13a	*CFX96 Touch Real-Time PCR System*	*RT-RPA*	*42 copies/reaction*	*1 h*	(Patchsung et al., 2020)
Cas12-based DETECTR	*Lateral flow visual readout*	*RT–LAMP*	*10 copies/μl*	*less than* 40 min	(Broughton et al., 2020)
CRISPR/Cas12a-NER	*Naked eye readout*	*RT-RAA*	*10 copies*	45 min	(Wang et al., 2020g)
Two-color RT-LAMP assay	*Plate scanner*	*RT-LAMP*	*Ct < 30*	30min	(Thi et al., 2020)
Single-tube assay based-Cas12a	*visualized using handheld UV lamp*	*RT–LAMP*	*30 copies/μL*	40 min	(Pang et al., 2020)
Nanopore targeted sequencing	*Oxford Nanopore MinION or GridION*	*RT-PCR*	*10 copies per reaction*	*6–10 h*	(Wang et al., 2020e)
Sensitive splint-based one-pot isothermal RNA detection	*Hidex Sense 425-301 microplate reader*	*NO*	*0.1 aM*	*30*–50 min	(Woo et al., 2020)
Our sensor	*Miniaturized smart device*	*RT-RAA*	*1 copies/mL*	40 min	Zhang et al. (2020)

Nonetheless, our proposed technique still has a few drawbacks. There are two main problems in our system at present. First, high-throughput detection cannot be carried out. Second, nucleic acid extraction, amplification and other steps cannot be integrated into the detection. However, considering the cost effect and storage time, the material cost for single detection of SARS-CoV-2 was less than 1.5 US dollars; the storage period of fluorescent nanoprobes and nucleic acid test strips could be maintained for at least 3 months at room temperature. Meanwhile, the simplicity and quickness of immunochromatography made this assay has the potential to be used in point-of-care detection. This finding showed that the CFNS assay method we proposed was a competitive substitute not only in technology but also in economy and practice, and it has the potential to be applied to point-of-care testing through continuous optimization in the future.

5. Conclusion

In this work we demonstrated that the QDMs labeled with FITC-antibody could act as a fluorescent signal that effectively detected SARS-CoV-2, resulting in a fast, sensitive, and specific biosensor for nucleic acid detection. The detection of different batches and placed for different periods confirmed that the fluorescent strip had a certain stability and could be placed at room temperature for 3 months. Through the detection of nucleic acids with different Ct values of RT-PCR, it is not difficult to find that our assay has a linear relationship with the Ct values measured by the gold standard, indicating that our detection system has the potential of quantitative detection. Moreover, the detection of a single copy of the SARS-CoV-2 nucleic acid could be achieved within 1 h (the detection limit of the RT-qPCR cycle threshold of clinical samples is up to 39). In summary, we successfully develop an immunochromatography technique based on QDMs and CRISPR/Cas13a for the detection of SARS-CoV-2, which is fast, sensitive, and specific with no need for complicated instruments as well as easy to operate.

Author contributions

Conceptualization: XW, FL and YY, Methodology: XW, FL and YY, Funding acquisition: XW, FL and YS, Project administration: XW and YY, Writing – original draft: QZ and JL, Writing – review & editing: XW, FL and YY, Specimen collection: QZ and LH, Nucleic acid extraction: GT, MS, KS and RS, Experimental operation: QZ and JL, Material preparation: YL, YS, YZ and XW.

Competing interests

All authors declare that they have no conflict of interest.

Declaration of competing interest

The authors declare that they have no known competing financial interests or personal relationships that could have appeared to influence the work reported in this paper.

Acknowledgements

This work was supported by Jiangsu Commission of Health M2020098 (XW); Fundamental Research Funds for the Central Universities KYZ202001(FL); The Priority Academic Program Development of Jiangsu Higher Education Institutions PAPD (FL); National Natural Science Foundation of China 32000028 (YS).

Appendix A. Supplementary data

Supplementary data to this article can be found online at https://doi.org/10.1016/j.bios.2022.113978.

References

Bai, Y., Yao, L., Wei, T., Tian, F., Jin, D.Y., Chen, L., Wang, M., 2020. JAMA 323 (14), 1406–1407.
Behera, B.C., Mishra, R.R., Thatoi, H., 2021. Biotechnol. Prog. 37 (1), e3078.
Broughton, J.P., Deng, X., Yu, G., Fasching, C.L., Servellita, V., Singh, J., Miao, X., Streithorst, J.A., Granados, A., Sotomayor-Gonzalez, A., Zorn, K., Gopez, A., Hsu, E., Gu, W., Miller, S., Pan, C.Y., Guevara, H., Wadford, D.A., Chen, J.S., Chiu, C.Y., 2020. Nat. Biotechnol. 38 (7), 870–874.
Bruchez Jr., M., Moronne, M., Gin, P., Weiss, S., Alivisatos, A.P., 1998. Science 281 (5385), 2013–2016.
CDC, 2020. https://www.cdc.gov/coronavirus/2019-ncov/lab/rt-pcr-detection-instructions.html. (Accessed December 2021).
Chaibun, T., Puenpa, J., Ngamdee, T., Boonapatcharoen, N., Athamanolap, P., O'Mullane, A.P., Vongpunsawad, S., Poovorawan, Y., Lee, S.Y., Lertanantawong, B., 2021. Nat. Commun. 12 (1), 802.
Chiara, M., D'Erchia, A.M., Gissi, C., Manzari, C., Parisi, A., Resta, N., Zambelli, F., Picardi, E., Pavesi, G., Horner, D.S., Pesole, G., 2021. Brief. Bioinform. 22 (2), 616–630.
Corman, V.M., Landt, O., Kaiser, M., Molenkamp, R., Meijer, A., Chu, D.K., Bleicker, T., Brunink, S., Schneider, J., Schmidt, M.L., Mulders, D.G., Haagmans, B.L., van der Veer, B., van den Brink, S., Wijsman, L., Goderski, G., Romette, J.L., Ellis, J., Zambon, M., Peiris, M., Goossens, H., Reusken, C., Koopmans, M.P., Drosten, C., 2020. Euro Surveill 25 (3).
Deiana, M., Mori, A., Piubelli, C., Scarso, S., Favarato, M., Pomari, E., 2020. Sci. Rep. 10 (1), 18764.
Ding, X., Yin, K., Li, Z., Lalla, R.V., Ballesteros, E., Sfeir, M.M., Liu, C., 2020. Nat. Commun. 11 (1), 4711.
Fozouni, P., Son, S., Diaz de Leon Derby, M., Knott, G.J., Gray, C.N., D'Ambrosio, M.V., Zhao, C., Switz, N.A., Kumar, G.R., Stephens, S.I., Boehm, D., Tsou, C.L., Shu, J., Bhuiya, A., Armstrong, M., Harris, A.R., Chen, P.Y., Osterloh, J.M., Meyer-Franke, A., Joehnk, B., Walcott, K., Sil, A., Langelier, C., Pollard, K.S., Crawford, E. D., Puschnik, A.S., Phelps, M., Kistler, A., DeRisi, J.L., Doudna, J.A., Fletcher, D.A., Ott, M., 2021. Cell 184 (2), 323–333 e329.
Hou, H., Wang, T., Zhang, B., Luo, Y., Mao, L., Wang, F., Wu, S., Sun, Z., 2020a. Clin. Transl. Immunology 9 (5), e01136.
Hou, T., Zeng, W., Yang, M., Chen, W., Ren, L., Ai, J., Wu, J., Liao, Y., Gou, X., Li, Y., Wang, X., Su, H., Gu, B., Wang, J., Xu, T., 2020b. PLoS Pathog 16 (8), e1008705.

Huang, C., Wang, Y., Li, X., Ren, L., Zhao, J., Hu, Y., Zhang, L., Fan, G., Xu, J., Gu, X., Cheng, Z., Yu, T., Xia, J., Wei, Y., Wu, W., Xie, X., Yin, W., Li, H., Liu, M., Xiao, Y., Gao, H., Guo, L., Xie, J., Wang, G., Jiang, R., Gao, Z., Jin, Q., Wang, J., Cao, B., 2020. Lancet 395 (10223), 497–506.
Karkan, S.F., Baladi, R.M., Shahgolzari, M., Gholizadeh, M., Shayegh, F., Arashkia, A., 2022. J. Virol. Methods 300, 114381.
Kevadiya, B.D., Machhi, J., Herskovitz, J., Oleynikov, M.D., Blomberg, W.R., Bajwa, N., Soni, D., Das, S., Hasan, M., Patel, M., Senan, A.M., Gorantla, S., McMillan, J., Edagwa, B., Eisenberg, R., Gurumurthy, C.B., Reid, S.P.M., Punyadeera, C., Chang, L., Gendelman, H.E., 2021. Nat. Mater. 20 (5), 593–605.
Laborde, D., Martin, W., Swinnen, J., Vos, R., 2020. Science 369 (6503), 500–502.
Mak, G.C., Cheng, P.K., Lau, S.S., Wong, K.K., Lau, C.S., Lam, E.T., Chan, R.C., Tsang, D. N., 2020. J. Clin. Virol. 129, 104500.
Meyerowitz, E.A., Richterman, A., Bogoch II, Low, N., Cevik, M., 2021. Lancet Infect. Dis. 21 (6), e163–e169.
Michalet, X., Pinaud, F.F., Bentolila, L.A., Tsay, J.M., Doose, S., Li, J.J., Sundaresan, G., Wu, A.M., Gambhir, S.S., Weiss, S., 2005. Science 307 (5709), 538–544.
Nicholson, K.G., 1992. Semin. Respir. Infect. 7 (1), 26–37.
Nicola, M., Alsafi, Z., Sohrabi, C., Kerwan, A., Al-Jabir, A., Iosifidis, C., Agha, M., Agha, R., 2020. Int. J. Surg. 78, 185–193.
Pang, B., Xu, J., Liu, Y., Peng, H., Feng, W., Cao, Y., Wu, J., Xiao, H., Pabbaraju, K., Tipples, G., Joyce, M.A., Saffran, H.A., Tyrrell, D.L., Zhang, H., Le, X.C., 2020. Anal. Chem. 92 (24), 16204–16212.
Patchsung, M., Jantarug, K., Pattama, A., Aphicho, K., Suraritdechachai, S., Meesawat, P., Sappakhaw, K., Leelahakorn, N., Ruenkam, T., Wongsatit, T., Athipanyasilp, N., Eiamthong, B., Lakkanasirorat, B., Phoodokmai, T., Niljianskul, N., Pakotiprapha, D., Chanarat, S., Homchan, A., Tinikul, R., Kamutira, P., Phiwkaow, K., Soithongcharoen, S., Kantiwiriyawanitch, C., Pongsupasa, V., Trisrivirat, D., Jaroensuk, J., Wongnate, T., Maenpuen, S., Chaiyen, P., Kamnerdnakta, S., Swangsri, J., Chuthapisith, S., Sirivatanauksorn, Y., Chaimayo, C., Sutthent, R., Kantakamalakul, W., Joung, J., Ladha, A., Jin, X., Gootenberg, J.S., Abudayyeh, O.O., Zhang, F., Horthongkham, N., Uttamapinant, C., 2020. Nat. Biomed. Eng. 4 (12), 1140–1149.
Pinheiro, T., Cardoso, A.R., Sousa, C.E.A., Marques, A.C., Tavares, A.P.M., Matos, A.M., Cruz, M.T., Moreira, F.T.C., Martins, R., Fortunato, E., Sales, M.G.F., 2021. ACS Omega 6 (44), 29268–29290.
Resch-Genger, U., Grabolle, M., Cavaliere-Jaricot, S., Nitschke, R., Nann, T., 2008. Nat. Methods 5 (9), 763–775.
Rothe, C., Schunk, M., Sothmann, P., Bretzel, G., Froeschl, G., Wallrauch, C., Zimmer, T., Thiel, V., Janke, C., Guggemos, W., Seilmaier, M., Drosten, C., Vollmar, P., Zwirglmaier, K., Zange, S., Wolfel, R., Hoelscher, M., 2020. N. Engl. J. Med. 382 (10), 970–971.
Thi, V.L.D., Herbst, K., Boerner, K., Meurer, M., Kremer, L.P., Kirrmaier, D., Freistaedter, A., Papagiannidis, D., Galmozzi, C., Stanifer, M.L., Boulant, S., Klein, S., Chlanda, P., Khalid, D., Barreto Miranda, I., Schnitzler, P., Krausslich, H.G., Knop, M., Anders, S., 2020. Sci. Transl. Med. 12 (556).
Wang, B., Li, R., Lu, Z., Huang, Y., 2020a. Aging (Albany N. Y.) 12 (7), 6049–6057.
Wang, C., Horby, P.W., Hayden, F.G., Gao, G.F., 2020b. Lancet 395 (10223), 470–473.
Wang, D., He, S., Wang, X., Yan, Y., Liu, J., Wu, S., Liu, S., Lei, Y., Chen, M., Li, L., Zhang, J., Zhang, L., Hu, X., Zheng, X., Bai, J., Zhang, Y., Zhang, Y., Song, M., Tang, Y., 2020c. Nat. Biomed. Eng. 4 (12), 1150–1158.
Wang, D., Hu, B., Hu, C., Zhu, F., Liu, X., Zhang, J., Wang, B., Xiang, H., Cheng, Z., Xiong, Y., Zhao, Y., Li, Y., Wang, X., Peng, Z., 2020d. JAMA 323 (11), 1061–1069.
Wang, M., Fu, A., Hu, B., Tong, Y., Liu, R., Liu, Z., Gu, J., Xiang, B., Liu, J., Jiang, W., Shen, G., Zhao, W., Men, D., Deng, Z., Yu, L., Wei, W., Li, Y., Liu, T., 2020e. Small 16 (32), e2002169.
Wang, M., Zhang, R., Li, J., 2020f. Biosens. Bioelectron. 165, 112430.
Wang, X., Zhong, M., Liu, Y., Ma, P., Dang, L., Meng, Q., Wan, W., Ma, X., Liu, J., Yang, G., Yang, Z., Huang, X., Liu, M., 2020g. Sci. Bull. 65 (17), 1436–1439.
WHO, 2020. https://www.who.int/docs/default-source/coronaviruse/wuhan-virus-assay-v1991527e5122341d99287a1b17c111902.pdf. (Accessed December 2021).
WHO, 2021. https://covid19.who.int/. (Accessed December 2021).
Williamson, E.J., Walker, A.J., Bhaskaran, K., Bacon, S., Bates, C., Morton, C.E., Curtis, H.J., Mehrkar, A., Evans, D., Inglesby, P., Cockburn, J., McDonald, H.I., MacKenna, B., Tomlinson, L., Douglas, I.J., Rentsch, C.T., Mathur, R., Wong, A.Y.S., Grieve, R., Harrison, D., Forbes, H., Schultze, A., Croker, R., Parry, J., Hester, F., Harper, S., Perera, R., Evans, S.J.W., Smeeth, L., Goldacre, B., 2020. Nature 584 (7821), 430–436.
Woo, C.H., Jang, S., Shin, G., Jung, G.Y., Lee, J.W., 2020. Nat. Biomed. Eng. 4 (12), 1168–1179.
Yuce, M., Filiztekin, E., Ozkaya, K.G., 2021. Biosens. Bioelectron. 172, 112752.
Zhang, F., Abudayyeh, O.O., Gootenberg, J.S., 2020. 8.
Zhu, N., Zhang, D., Wang, W., Li, X., Yang, B., Song, J., Zhao, X., Huang, B., Shi, W., Lu, R., Niu, P., Zhan, F., Ma, X., Wang, D., Xu, W., Wu, G., Gao, G.F., Tan, W., 2020. China novel coronavirus, I., research, T. N. Engl. J. Med. 382 (8), 727–733.